Chapter VI

Effective photocatalytic activity of nanoscale Eu^{3+}:$GdVO_4$ on Congo Red (CR) dye

Much interest in the development of newer methods/techniques has been encouraged in recent years for tackling environmental remediation of pollutants released through industrial plants and human activity [1]**.** To be mentioned, highly toxic and carcinogenic azo dyes constitute ~50-70% of all organic dyes used in textile based industries and mills [1, 2]. Following an attempt to degrade them, these dyes form harmful byproducts via processes, such as oxidation, hydrolysis, or other regular chemical reactions, leading to secondary problems [3]. It was known that *Congo red* (CR), the first anionic synthetic azo dye is relatively more stable than other dyes with two azo chromophores due to its complex aromatic structure containing one central biphenyl group and two symmetric naphthalenic groups as illustrated in **FIGURE 6.1**. A great deal of reports can be found in the literature that describe numerous techniques being applied for degradation of azo dyes, including- ion exchange, membrane separation or nano filtration, usage of activated carbon, irradiation, electro kinetic chemical coagulation/flocculation, electrochemical destruction, ozonation and photochemical degradation [4-9]. Nevertheless, most of the aforementioned conventional techniques for photocatalysis are not eco
nomically viable as they require high-end technological interventions, and may exhibit severe disadvantages from making them effective against all-dye types, production of sludge including formation of unwanted byproducts [6]. In this regard, potential use of nanocatalysts is worth investigating which could display efficient catalytic properties in water and wastewater treatment [10**]** and splitting of water [11, 12].

Theoretically, $GdVO_4$ exhibits the desired position of the band edges thereby promising a potential photocatalytic agent with higher ability to generate hydrogen from water or water/alcohol solutions via photoexcited reactions which could be excited using visible light as well [13, 14]**.** Photocatalytic behavior of metal-oxide nanosystem is well defined but only a limited number of reports are available that deal with photocatalytic activity of $ReVO_4$ nanosystem [15-18].

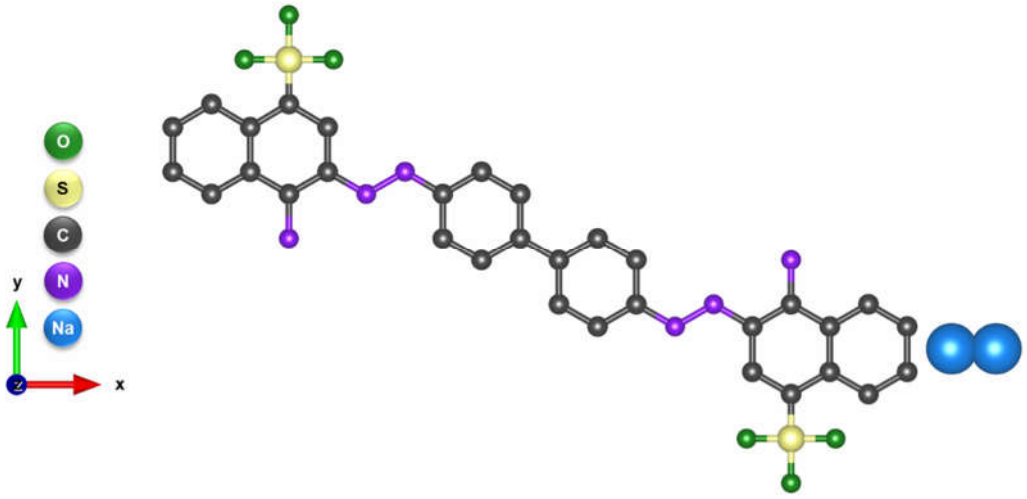

FIGURE 6.1 Molecular structure of Congo Red prepared using *Vesta*®.

A superior photocatalysis of azo based dyes has been speculated recognizing that the $GdVO_4$ nanosystem comes with an excellent capability to generate hydrogen from water **[14, 19].** Reports can be found In literature that deal with possible enhancement of photocatalytic activity of a nanosystem following inclusion of metal ions as dopants **[20]**. RE ions as dopants were also shown to increase the activity against azo dyes under visible light illumination **[21]**. In particular, effects of europium doping on the photocatalytic behavior of AVO_4 systems has been evaluated earlier and the observed augmentation in photocatalytic behavior was ascribed due to the effective spatial separation of electron (e)–hole(h) following inclusion of dopants into the system **[22]**. It can thus be speculated that RE ion doped in RE photocatalysts could prove to be an efficient way to increase the photocatalytic activity. In this chapter, we highlight the photocatalytic performance of the as-derived nanocatalysts against azo dye-CR.

6.1 Photocatalytic studies on CR dye through characteristic absorbance spectra

FIGURE 6.2. (a) shows the characteristic absorbance spectra of CR dye at varied concentrations. The band centering around ~340 nm is assigned to π–π* transition of the aromatic ring while the most intense band ~496 nm is attributed to the n–

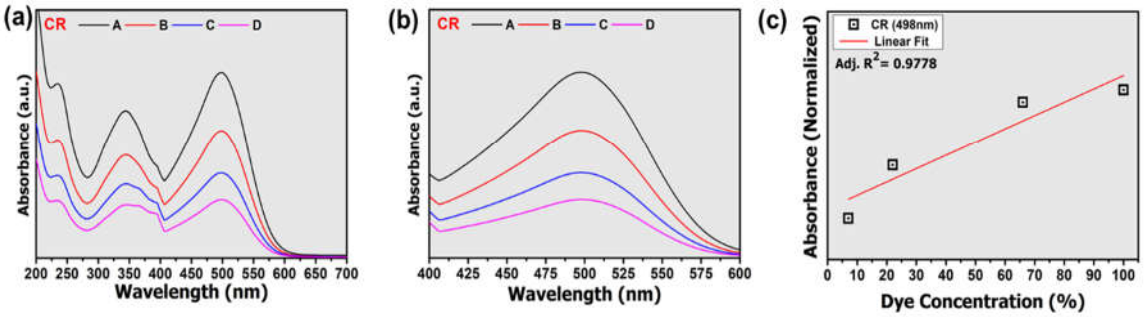

FIGURE 6.2: (a) Absorbance spectra of Congo Red (CR) dye revealing characteristic peaks at varying concentrations (A- 100%, B- 66%, C- 22%, D- 7%). (b) Normalized absorbance spectra of CR and (c) standard linear plot for determining the dye degradation %.

π* transition of the lone pair of N atom of the chromophoric –N═N– azo moiety **[23]**. Dye degradation is monitored by determining the decrement of absorbance of ~496 nm peak primarily indicating –N═N– bond cleavage.

In order to determine the photocatalytic activity of GdV and EuGdV towards degradation of CR dye, a stock dye solution is prepared with 1 mg of CR added to 200 ml of DI water. The nanocatalyst is then introduced into the solution suitably and the UV-Vis absorbance spectra were recorded at regular intervals and up to 3 h. For a better comparison of the effect of Eu^{3+} dopants in the enhancement of the photocatalytic activity, the amount of photocatalysts, i.e. GdV and 3% EuGdV were kept same for both the studies. To be specific, stock photocatalyst solution is prepared adding 20mg of catalyst in 1.5 ml D/W. Then, 400 µl of photocatalyst is added from the stock photocatalyst solution into 100ml of CR stock dye solution. The resultant suspension is sonicated for 5 min and then stirred in the dark for 30–45 min to ensure the adsorption/desorption equilibrium on the nano-photocatalyst surface prior to irradiation. UV or visible irradiation (as required) with a distance of about 15 cm between the light source and the reaction mixture has been employed as per the case. For proper assessment, digital photographs of the degradation steps are captured. The dye degradation at the irradiation time intervals can be quantified using the following equation:

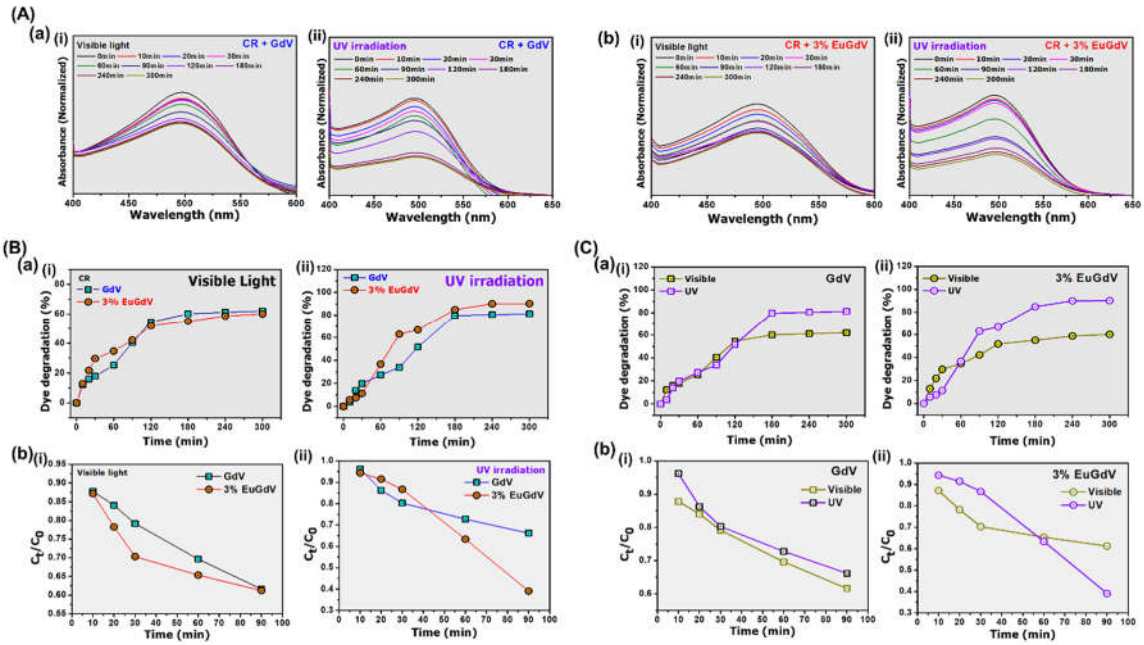

FIGURE 6.3: Photocatalytic behaviour of nanocatalyst against CR dye: (A) progressive optical absorption features (a) GdV, and (b) EuGdV with (i) visible light, and (ii) UV light illumination. (B) A comparative view on dye degradation in terms of (a) percentage, and (b) relative concentration with time progression. (C) comparative account on photocatalytic effeciencies of nanocatalysts under visible and UV exposure.

$$Dye\ degradation\ \% = \left(\frac{C_0 - C_t}{C_0}\right) \times 100 \qquad (6.1)$$

where, C_0 and C_t represent concentration of the dye solution before and after irradiation, and determined from a standard curve of absorbance values obtained from known concentrations of CR dye (**FIGURE. 6.2).**

6.2 Dye removal efficiency of EuGdV nanocatalyst under white light and UV light illumination

In **FIGURE 6.3 (A),** the absorbance quenching of CR is displayed treated with (a) GdV, and (b) 3% EuGdV under both the irradiations i.e., (i) visible and (ii) UV. It is noteworthy that reports can be found suggesting improvement of photocatalytic activity of the doped nanosystem upon increasing Eu^{3+} concentration, however, the enhancement saturates for dopant level beyond ~1.46 wt% **[24].** It must thus be noted that excess Eu^{3+} species may either act as

recombination centers or covers of active sites on the catalyst surfaces. Consequently, higher Eu^{3+} concentration results in the confinement of Eu^{3+} on the surface of catalysts, and the possibility for the trapped electrons to recombine with the holes increases eventually. In such case, efficiency of charge separation is reduced **[22]**. In addition, it must be noted that Eu^{3+} concentration above ~5mol% attracts quenching effects that would occur due to energy transfer between neighbouring Eu^{3+} ions **[25]**. Such an energy transfer reduces the efficacy of UV excitation and can result in lower photocatalytic performance. In order to avoid reduction of charge separation due to excess Eu^{3+} in the system leading to increased energy transfer and thus poorer photocatalytic activity, ~3mol% EuGdV nanosystem was purposefully chosen for photocatalytic studies. In fact, we observed an excellent photocatalytic behavior of the nanocatalyst that leads to an efficient degradation of the target CR molecules within 120 min., beyond which the process is slowed down. The digital photographs of the dye illustrating progressive discoloration after 120 min of treatment time under both the visible light and UV irradiation can be viewed in **FIGURE.6.4**.

The variation in percentage of dye degradation for both the nanosystems under bright light illumination and UV lightexposure can be found in **FIGURE 6.3(B)**. For photocatalytic behavior observed under visible light (**FIGURE 6.3 (B)(a)(i),** both GdV and EuGdV displayed similar results with an effective dye degradation upto ~60% after a treatment for 300 min. For the initial 120 min, the activity progressed steadily following which the behavior gets a saturative trend. Interestingly, upon treatment with UV light (**FIGURE 6.3(B)(a) (ii)),** the photodegradation efficiency shoots up to ~80% for GdV, and even as high as ~91.8% for 3% EuGdV nanocatalyst. The kinetics of the CR-dye degradation process is shown in **FIGURE 6.3(B)(b**) and can be best described through Langmuir–Hinshelwood (L-H) model, expressed in the form of a first-order reaction considering a dilute solution [26]:

$$C_t = C_0 e^{-kt} \qquad (6.2)$$

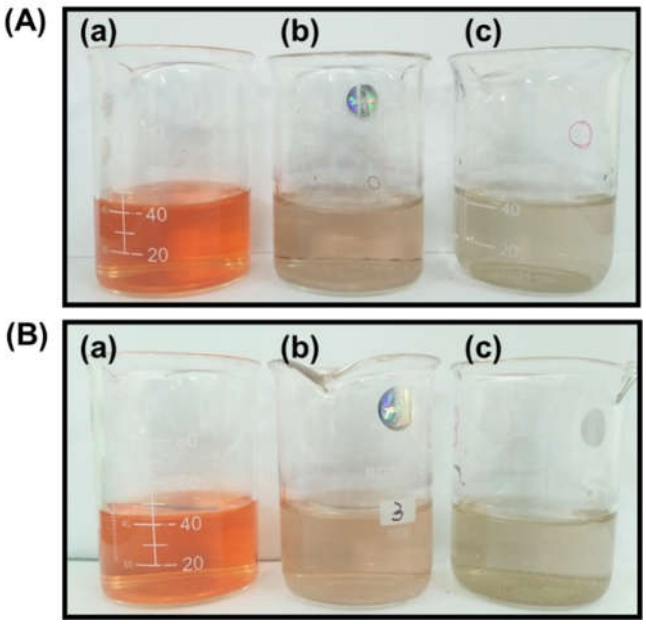

FIGURE 6.4. Dye degradation process of CR upon 120 minutes of treatment with (A) GdV and (B) 3%EuGdV under (b) bright light illumination and (c) UV irradiation. (A)(a) and (B)(a) displays images for CR dyes left untreated for the same amount of time.

In Eqn.6.2, 't' is the irradiation time while 'k' is pseudo-first order rate constant. The rate constant was predicted from the plot of (C_t/C_0) versus '*t*' shown in the insets of Fig. 6.3 (A), (B)- (b, c). To be mentioned, with visible light irradiation, the rate constants were found similar for both the undoped (GdV) and doped (EuGdV) nanosytems but *k* value gets augmented considerably from ~0.034 min^{-1} to ~0.071 min^{-1} under UV light illumination. Such an increment in rate constant upon Eu incorporation is unprecedented, suggesting that the Eu^{3+} dopant ions are proficient in improving photocatalytic activity under UV exposure. Available reports suggest rate constants, for degradation of azo dyes using $ReVO_4$ nanosystem to be 0.064 min^{-1} ($CeVO_4$), 0.066 min^{-1} ($PrVO_4$) and 0.058 min^{-1} ($NdVO_4$) [27]. Our observations in case of 3% EuGdV is comparable to the degradation rate constant for commercially available TiO_2/Degussa P-25 (*k*=0.079 min^{-1}) thereby confirming potential use for azo dye degradation. Based on the available literature, description of origin of photocatalytic activity by a nanosystem involves various parameters, *viz.* high surface area, finite value of

band gap, crystallinity of the photocatalyst, presence of defect states (typically, oxygen based) etc. Previously, lanthanides have shown substantial enhancement in photocatalytic activity under visible light irradiation as well, however the prime mechanism responsible has not yet been established [28]. A comprehensive and comparative overview, focusing on photocatalytic performance of $REVO_4$ as nano-photocatalyst against CR and other dye types can be found in **TABLE 1**. In general, a photocatalytic reaction proceeds via several steps [29-31]:

(a) *Photoexcitation*: Depending on the source of illumination and bandgap of the catalyst used, photons of definite energy are utilized in exciting the electrons of the valence band (VB) to jump into the conduction band (CB).

(b) *Charge separation*: The photoexciation process leads to generation of electron-hole pairs with positive holes (h^+) in VB and electrons (e^-) in the CB [32, 33].

(c) *Migration:* A share of the photogenerated pairs distributes out to the photocatalyst surface wherein they participate in chemical reactions with the highly reactive hydroxyl radicals and superoxide radical ions by oxidizing adsorbed organic contaminants and water adsorbed on the photocatalyst surface [31, 32].

(d) *Recombination*: Recombination is a very quick process, and thus efficacy of the photocatalysis relies on the amount of reactants adsorbed on the photocatalyst surface. Holes have strong oxidizing capacity and can produce highly reactive hydroxyl radical and superoxide radical ions by oxidizing adsorbed organic contaminants and water (adsorbed on the photocatalyst surface) [31, 32]. Consequently, the super reactive radicals facilitate dye degradation thereby generates wide ranging intermediates, which are known to completely mineralize into carbon dioxide, water, ammonium and nitrate ion [34].

TABLE 1. A comparative view highlighting photocatalytic performance of $REVO_4$ and other systems as nanophotocatalyst against different dye types

Sl. no	Target dye/ contaminant	Material	Illumination source	Degradation % - Treatment time	Ref
1	Congo red	$CuInSe_2$–ZnO nanocomposites	UV	99.8% - 90min	[31]
			Visible	80.3%- 120min	
2		Ba/Alg/CMC/TiO_2 composite	Solar light	91.5 %-240min	[34]
3		Zn-doped $CdTiO_3$/TiO_2	Solar light	90%- 15 min	[35]
4		$PbTiO_3$	Visible	92%- 150min	[36]
5		TiO_2	Multi lamp photoreactor	74%- 120min	[37]
		CNBF/TiO_2	Multi lamp photoreactor	83%- 120min	
6	Malachite Green	$GdVO_4$	Visible	96.2%- 50min	[32]
	Rhodamine Blue			89.2%-50min	
	Methylene Blue			87.8%-50min	
7	Rhodamine Blue	$GdVO_4$	Solar light	69%- 360min	[18]
8	Acetone	$GdVO_4$-V_2O_5	Visible	95.5%-180min	[13]
9	Methyl orange	$GdVO_4$	UV light	85% -70 min	[38]
10	**Congo red**	**Eu^{3+}:$GdVO_4$**	**UV light and visible light**	**91.8%- 180 min**	**This work**

The reaction steps involved in the entire photocatalytic response is detailed below:

$$GdV \xrightarrow{h\upsilon} GdV(e_{CB}^{-} + h_{VB}^{+}) \quad (i)$$

$$GdV(h_{VB}^{+}) + H_2O \text{ or } OH^{-} \rightarrow H^{+} + OH^{\cdot} \quad (ii)$$

$$GdV(e_{CB}^{-}) + O_2 \rightarrow O^{2-} \quad (iii)$$

$$O^{2-} + H^{+} \rightarrow HO_2^{\cdot} \quad (iv)$$

$$2HO_2^{\cdot} \rightarrow H_2O_2 + O_2 \quad (v)$$

$$H_2O_2 \rightarrow 2OH^{-} \quad (vi)$$

Consequently,

$$CR\ dye + O_2^{\cdot -} + OH^{\cdot} \rightarrow intermediate\ products \rightarrow CO_2 + H_2O + NO_3^{-} + NH_4^{+} \quad (vii)$$

K. Hubenko *et. al.* has reported that Eu^{3+}:$GdVO_4$nanoparticles have a great potential in generating reactive oxygen species in aqueous solutions containing azo dyes [39]. Furthermore, surface oxygen coordination defects of V atoms are known to activate the water dissociative adsorption thereby creating radical ions. It is worth mentioning here that the highest occupied state of the RE- vanadates energy levels are located above occupied O2*p* orbitals of the adsorbed water molecules, enabling them to generate hydrogen from water dissociation [40]. Optically excited transitions involved in $GdVO_4$ *viz.* from occupied valence band to unoccupied Gd 4*f* band and O2*p* to V3*d*, promotes hydrogen generation in aqueous media [31]. For more clarity of the effect of irradiation type in enhancing as regards the photocatalytic activity of both the polyhedral nanosystems, we refer to Fig 6.3(C)(a). Augmented dye degradation process upon UV irradiation is quite evident for (i) GdV and (ii) 3% EuGdV. Interestingly, the observation is more pronounced in case of 3% EuGdV with an efficiency as high as 91.8%.

6.2.2 Effect of Eu^{3+} doping in augmentation of photocatalytic activity of GdV

Our observations suggest that incorporation of Eu^{3+} as dopant into the GdV nanosystem would make a better photocatalytic agent. It is noteworthy that for both the photocatalysts, the synthesis as well as treatment conditions were same. The only difference lies in the presence of Eu^{3+} as dopant in the system. Inclusion of dopants into the system introduces various changes in the host system, both

physical as well as optical. It has been reported earlier that an increased porosity due to doping can augment the photocatalytic activity [41]. In our case, however, the porosity was slightly lowered due to inclusion of dopants (4.64% -GdV and 4.58% - 3% EuGdV). Thus the change in porosity is not considered the only criterion for augmenting the photocatalytic activity observed. It is worth mentioning that the UV irradiation wavelength is closer to absorbance peak of Eu^{3+} which facilitates photoexcitation events efficiently resulting in profound generation of *e-h* pairs. The increased activity of photocatalyst upon Eu dopant has been proposed to occur via the trapping of photogenerated electrons within the catalyst, thereby reducing the extent of *e-h* recombination known for diminishing the activity [42]. Such electron trapping by Eu^{3+} dopant reduces the electron–hole recombination rate in the reaction and therefore additional holes are available for the redox reactions involved in the photodegradation of the dye [43]. The CT processes involving Eu–O and general intra *f* transitions due to Eu^{3+} incorporation into the vanadate matrix, further enables greater generation of more reactive species that facilitates decomposition and decolorization of CR under UV light. Enhanced photocatalytic activity of 3% EuGdV in our observation can be explained citing the organic contaminant, CR, disintegrated eventually following production of CO_2, water and other byproducts.

6.3 Concluding remarks

The CR dye was apparently degraded upto an extent of ~91.8% by Eu^{3+}:$GdVO_4$ nanocatalyst, possibly to other aromatic species, with noticeable discoloration effect. Notably, the rate constant gets doubled with the inclusion of dopant into the host. Photocatalytic steps and associated mechanisms are also elucidated. The quantification and toxicity tests of these intermediates, which promise to be an interesting area of research would provide vital information regarding environmental remediation and safe use of the catalytic agent. A better understanding of the photocatalytic processes and the operative conditions with alternative candidates of the photocatalyst could offer great opportunities for its

industrial relevance targeting environmental pollutants and organic contaminants.

Bibliography

[1] Erdemoğlu, S., Aksu, S.K., Sayılkan, F., Izgi, B., Asiltürk, M., Sayılkan, H., Frimmel, F., and Güçer, Ş., Photocatalytic degradation of Congo Red by hydrothermally synthesized nanocrystalline TiO_2 and identification of degradation products by LC–MS. *Journal of Hazardous Materials*, 155(3):469-476, 2008.

[2] Molinari, R., Pirillo, F., Falco, M., Loddo, V., and Palmisano, L., Photocatalytic degradation of dyes by using a membrane reactor. *Chemical engineering and processing: process intensification*, 43(9):1103-1114, 2004.

[3] Sakkas, V.A., Islam, M.A., Stalikas, C., and Albanis, T.A., Photocatalytic degradation using design of experiments: a review and example of the Congo red degradation. *Journal of Hazardous Materials*, 175(1-3):33-44, 2010.

[4] Varga, M., Kopecký, D., Kopecká, J., Křivka, I., Hanuš, J., Zhigunov, A., Trchová, M., Vrňata, M., and Prokeš, J., The ageing of polypyrrole nanotubes synthesized with methyl orange. *European Polymer Journal*, 96:176-189, 2017.

[5] Rattanapan, S., Srikram, J., and Kongsune, P., Adsorption of methyl orange on coffee grounds activated carbon. *Energy Procedia*, 138:949-954, 2017.

[6] Jha, A.K. and Chakraborty, S., Photocatalytic degradation of Congo Red under UV irradiation by zero valent iron nano particles (nZVI) synthesized using Shorea robusta (Sal) leaf extract. *Water Science and Technology*, 82(11):2491-2502, 2020.

[7] Namasivayam, C. and Kavitha, D., Removal of Congo Red from water by adsorption onto activated carbon prepared from coir pith, an agricultural solid waste. *Dyes and pigments*, 54(1):47-58, 2002.

[8] Chakraborty, S., Purkait, M., DasGupta, S., De, S., and Basu, J., Nanofiltration of textile plant effluent for color removal and reduction in COD. *Separation and Purification Technology*, 31(2):141-151, 2003.

[9] Etemadinia, T., Barikbin, B., and Allahresani, A., Removal of Congo red dye from aqueous solutions using $ZnFe_2O_4/SiO_2$/Tragacanth gum magnetic nanocomposite as a novel adsorbent. *Surfaces and Interfaces*, 14:117-126, 2019.

[10] Ismail, A., Ibrahim, I., Ahmed, M., Mohamed, R., and El-Shall, H., Sol–gel synthesis of titania–silica photocatalyst for cyanide photodegradation. *Journal of Photochemistry and Photobiology A: Chemistry*, 163(3):445-451, 2004.

[11] Xu, H., Shang, H., Wang, C., Jin, L., Chen, C., Wang, C., and Du, Y., Three-dimensional open $CoMoO_x/CoMoS_x/CoS_x$ nanobox electrocatalysts for efficient oxygen evolution reaction. *Applied Catalysis B: Environmental*, 265:118605, 2020.

[12] Xu, H., Shang, H., Jin, L., Chen, C., Wang, C., and Du, Y., Boosting electrocatalytic oxygen evolution over Prussian blue analog/transition metal dichalcogenide nanoboxes by photo-induced electron transfer. *Journal of Materials Chemistry A,* 7(47):26905-26910, 2019.

[13] He, Y., Cai, J., Li, T., Wu, Y., Lin, H., Zhao, L., and Luo, M., Efficient degradation of RhB over $GdVO_4$/g-C_3N_4 composites under visible-light irradiation. *Chemical engineering journal*, 215:721-730, 2013.

[14] Oshikiri, M., Ye, J., and Boero, M., The role of Ni-based cocatalyst in inhomogeneous RVO_4 photocatalyst systems (R= Y, Gd). *The Journal of Physical Chemistry C,* 118(24):12845-12854, 2014.

[15] Karimi, P., Hui, K., and Komal, K., Hydrothermal synthesis of yttrium orthovanadate (YVO4) and its application in photo catalytic degradation ofsewage water. *Iranian Journal of Materials Science and Engineering*, 7(3):25-30, 2010.

[16] Xu, H., Wang, H., and Yan, H., Preparation and photocatalytic properties of YVO_4 nanopowders. *Journal of hazardous materials*, 144(1-2):82-85, 2007.

[17] Klochkov, V., Comparative analysis of photocatalytic activity of aqueous colloidal solutions of ReVO: Eu^{3+} (Re= La, Gd, Y), $CePO_4$: Tb, CeO_2 and C_{60}. *Journal of Photochemistry and Photobiology A: Chemistry*, 310:128-133, 2015.

[18] Bai, Y., Ding, Y.M., and Li, Z.M. Photocatalytic water splitting and photocatalytic degradation in aqueous $GdVO_4$ suspensions under simulated solar irradiation. in *Advanced Materials Research*, Vol. 873. 571-574: Trans Tech Publ, 2014.

[19] Mazierski, P., Sowik, J., Miodyńska, M., Trykowski, G., Mikołajczyk, A., Klimczuk, T., Lisowski, W., Nadolna, J., and Zaleska-Medynska, A., Shape-controllable synthesis of $GdVO_4$ photocatalysts and their tunable properties in photocatalytic hydrogen generation. *Dalton Transactions*, 48(5):1662-1671, 2019.

[20] Lim, H. and Rawal, S.B., Integrated Bi_2O_3 nanostructure modified with Au nanoparticles for enhanced photocatalytic activity under visible light irradiation. *Progress in Natural Science: Materials International*, 27(3):289-296, 2017.

[21] Xie, Y., Yuan, C., & Li, X., Photosensitized and photocatalyzed degradation of azo dye using Lnn+-TiO_2 sol in aqueous solution under visible light irradiation. *Materials Science and Engineering: B*, 117(3), 325-333, 2005.

[22] Zhang, A. and Zhang, J., Effects of europium doping on the photocatalytic behavior of $BiVO_4$. *Journal of Hazardous Materials*, 173(1-3):265-272, 2010.

[23] Wang, L., Li, J., Wang, Z., Zhao, L., and Jiang, Q., Low-temperature hydrothermal synthesis of α-Fe/Fe_3O_4 nanocomposite for fast Congo red removal. *Dalton Transactions*, 42(7):2572-2579, 2013.

[24] Xu, Z., Kang, X., Li, C., Hou, Z., Zhang, C., Yang, D., Li, G., and Lin, J., Ln^{3+} (Ln= Eu, Dy, Sm, and Er) ion-doped YVO_4 nano/microcrystals with multiform

morphologies: hydrothermal synthesis, growing mechanism, and luminescent properties. *Inorganic Chemistry*, 49(14):6706-6715, 2010.

[25] Wei, Z., Sun, L., Liao, C., Yin, J., Jiang, X., Yan, C., and Lü, S., Size-dependent chromaticity in YBO_3: Eu nanocrystals: correlation with microstructure and site symmetry. *The Journal of Physical Chemistry B*, 106(41):10610-10617, 2002.

[26] Hazarika, S.J. and Mohanta, D., Inorganic fullerene-type WS_2 nanoparticles: processing, characterization and its photocatalytic performance on malachite green. *Applied Physics A*, 123(5):381, 2017.

[27] Mahapatra, S., Madras, G., and Guru Row, T., Synthesis, characterization and photocatalytic activity of lanthanide (Ce, Pr and Nd) orthovanadates. *Industrial & Engineering Chemistry Research*, 46(4):1013-1017, 2007.

[28] Sobhani-Nasab, A. and Behpour, M., Synthesis, characterization, and morphological control of $Eu_2Ti_2O_7$ nanoparticles through green method and its photocatalyst application. *Journal of Materials Science: Materials in Electronics*, 27(11):11946-11951, 2016.

[29] Li, H., Yin, S., Wang, Y., and Sato, T., Efficient persistent photocatalytic decomposition of nitrogen monoxide over a fluorescence-assisted $CaAl_2O_4$:(Eu, Nd)/(Ta, N)-codoped TiO_2/Fe_2O_3. *Applied Catalysis B: Environmental*, 132:487-492, 2013.

[30] Palanisamy, B., Babu, C., Sundaravel, B., Anandan, S., and Murugesan, V., Sol–gel synthesis of mesoporous mixed Fe_2O_3/TiO_2 photocatalyst: application for degradation of 4-chlorophenol. *Journal of Hazardous Materials*, 252:233-242, 2013.

[31] Bagheri, M., Mahjoub, A.R., and Mehri, B., Enhanced photocatalytic degradation of congo red by solvothermally synthesized $CuInSe_2$–ZnO nanocomposites. *RSC Advances*, 4(42):21757-21764, 2014.

[32] He, A., Feng, L., Liu, L., Peng, J., Chen, Y., Li, X., Lu, W., and Liu, J., Design of novel egg-shaped $GdVO_4$ photocatalyst: a unique platform for the

photocatalyst and supercapacitors applications. *Journal of Materials Science: Materials in Electronics*, 31(16):13131-13140, 2020.

[33] Hoffmann, M.R., Martin, S.T., Choi, W., and Bahnemann, D.W., Environmental applications of semiconductor photocatalysis. *Chemical Reviews*, 95(1):69-96, 1995.

[34] Thomas, M., Natarajan, T.S., Sheikh, M.U.D., Bano, M., and Khan, F., Self-organized graphene oxide and TiO_2 nanoparticles incorporated alginate/carboxymethyl cellulose nanocomposites with efficient photocatalytic activity under direct sunlight. Journal of Photochemistry and Photobiology A: Chemistry, 346:113-125, 2017.

[35] Moradzadeh, A., Mahjoub, A., Sadjadi, M.S., Sadr, M.H., and Farhadyar, N., Investigation on synthesis, characterization and photo catalytic degradation of Congo red by Zn-doped $CdTiO_3$/TiO_2. *Polyhedron*, 170:404-411, 2019.

[36] Bhagwat, U.O., Wu, J.J., Asiri, A.M., and Anandan, S., Photocatalytic degradation of congo red using $PbTiO_3$ nanorods synthesized via a sonochemical approach. *ChemistrySelect*, 3(42):11851-11858, 2018.

[37] Ramakrishnan, R., Kalaivani, S., Joice, J.A.I., and Sivakumar, T., Photocatalytic activity of multielement doped TiO_2 in the degradation of congo red. *Applied Surface Science*, 258(7):2515-2521, 2012.

[38] Vosoughifar, M., Nanocrystalline $GdVO_4$: Synthesis, characterization, optical and photocatalytic properties. *Journal of Materials Science: Materials in Electronics,* 28(8):6119-6124, 2017.

[39] Hubenko, K., Yefimova, S., Tkacheva, T., Maksimchuk, P., Borovoy, I., Klochkov, V., Kavok, N., Opolonin, O., and Malyukin, Y., Reactive oxygen species generation in aqueous solutions containing $GdVO_4$:Eu^{3+} nanoparticles and their complexes with methylene blue. *Nanoscale Research Letters*, 13(1):1-9, 2018.

[40] Oshikiri, M., Boero, M., Matsushita, A., and Ye, J., Water adsorption onto Y and V sites at the surface of the YVO 4 photocatalyst and related electronic properties. *The Journal of Chemical Physics*, 131(3):034701, 2009.

[41] Sukumar, M., Kennedy, L.J., Vijaya, J.J., Al-Najar, B., and Bououdina, M., Structural, magnetic and catalytic properties of $La_{2-x}Ba_xCuO_4$ ($0 \leq x \leq 0.5$) perovskite nanoparticles. *Ceramics International*, 44(15):18113-18122, 2018.

[42] Borgarello, E., Kiwi, J., Graetzel, M., Pelizzetti, E., and Visca, M., Visible light induced water cleavage in colloidal solutions of chromium-doped titanium dioxide particles. *Journal of the American Chemical Society*, 104(11):2996-3002, 1982.

[43] Xu, J., Ao, Y., Fu, D., and Yuan, C., A simple route for the preparation of Eu, N-codoped TiO_2 nanoparticles with enhanced visible light-induced photocatalytic activity. *Journal of Colloid and Interface Science*, 328(2):447-451, 2008.